https://doi.org/10.2352/ISSN.2470-1173.2018.11.IMSE-326

A Distance Measurement Method Using A Time-of-Flight CMOS Range Image Sensor with 4-Tap Output Pixels and Multiple Time-Windows

Kohei Yamada† Komazawa Akihito† Taishi Takasawa† Keita Yasutomi† Keiichiro Kagawa† and Shoji Kawahito†
† Research Institute of Electronics, Shizuoka University, 3-5-1 Johoku, Naka-ku, Hamamatsu, Shizuoka, 432-8011, Japan
E-mail: kyama@idl.rie.shizuoka.ac.jp TEL: +81-53-478-1342 FAX: +81-53-412-5481

Abstract

In this study, advanced range measurement method using a TOF sensor with 4-tap output pixels and small-duty short light pulse is presented. A CMOS TOF range imager with pinned-photodiode high-speed charge modulator pixels using lateral electric field (LEF) control has been implemented by a 0.11-μm CIS process with high near infrared sensitivity. In order to improve the range resolution while maintaining the measurable range, multiple time-windows are used for range measurements. Compared with the conventional single time window, the use of N time-windows theoretically improve the range resolution by a factor of $N^{1.5}$ if the back ground light shot noise is dominant. In the measurement for N=2, the range resolution is improved by a factor of 2.8 compared with the case of N=1 while maintaining the same distance range.

Introduction

Indirect-type Time-of-Flight (TOF) range imagers recently have been paid much attentions to applications for outdoor use, particularly for smart devices, robot eyes, VR/AR, security systems and automobiles. Various Indirect-type TOF range imagers have been reported [1-8], though, the tolerance to large ambient light is not always well considered. In general, there are two modulation methods of light; continuous wave (CW) and short pulse (SP) modulations. The CW modulation is better for high linearity of range measurements, and by increasing the modulation frequency, the CW modulation has high range resolution if the ambient light is small enough. However, in the CW modulation, because the duty-ratio of the modulated light is 50%, the tolerance to ambient light is hard to be comparable of better than that of the indirect-type TOF range imagers which use short light pulse where the light energy is concentrated at very short instance. Concerning the tolerance to the ambient light, the SP modulation method in the indirect TOF range imaging should has a better performance than the CW method. However, in the conventional SP modulation method, there is a tradeoff between the range resolution and maximum measurable range.

To address the trade-off problem between maximum measurement range and range resolution, in this paper, a CMOS TOF range imaging technique using the SP modulation, multiple (>2)-tap demodulation pixels and a range-shifting operation is presented. A 4-tap lateral electric field charge modulator (LEFM) pixels with high-speed charge draining structure based on photodiode CMOS image sensor technology [9,10] is used. The proposed lock-in pixel structure using lateral electric field (LEF) control is suitable for implementing a multiple-tap charge modulator while achieving high-speed charge transfer and high demodulation contrast for high time resolution [12]. In the conventional range measurement method, a single time window is used for range measurement. In the proposed technique, switchable multiple time windows based on the range-shifting operation and automatic range switching with thresholding to the multi-tap pixel outputs are used. The effectiveness of the proposed technique is experimentally confirmed by applying the technique to an implemented CMOS TOF imager.

Range Measurement with Double Light Pulse

The timing diagram for range shift operation with a small duty-ratio double light pulse is shown in Fig. 1. The gate pulse width of G1, G2, G3 and G4 is given by $R_D T_C$, where T_C is the cycle time and R_D is duty ratio of the gate pulse to the cycle time. Then, the gate pulse width of GD is given by $(1-4R_D)\,T_C$. The signal light pulse width and the time of flight of the received light are denoted by T_0 and T_d, respectively. The signals from FD1, FD2, FD3 and FD4 are denoted by S1, S2 S3 and S4, respectively. In TOF method, the equation for estimating the range is given by

$$L = \frac{1}{2} c T_d \tag{1}$$

where L is the range, c is the speed of light.

In the case of received light (2) in Fig. 1, the difference of the amount of charges between the two FDs (FD1, FD2) reflects the time-of-flight of light pulse T_d. The range is calculated by the TOF-dependent charges. During G1 is activated and the other gates are deactivated, a part of the signal light pulse is received, and the signal charge Q_1 is stored in FD1. The Q_1 is expressed as

$$Q_1 = I_S(T_0 - T_d) \tag{2}$$

where I_S is the photo current generated by the signal light pulse. In the next phase where G2 gates are activated and the other gates are deactivated, the rest part of the light pulse is received and the signal charge Q_2 stored in FD2 is expressed as

$$Q_2 = I_S T_d \tag{3}$$

If the background light exists, Eq. 2 and Eq. 3 are modified as

$$Q_1 = I_S(T_0 - T_d) + I_{BL} R_D T_C \tag{4}$$

$$Q_2 = I_S T_d + I_{BL} R_D T_C \tag{5}$$

where I_{BL} is photo current generated by the background light and $R_D T_C$ is the gate pulse width.

In order to cancel the background light, FD3 and FD4 are used for taking background light charges only. The electrons generated by background light are transferred from pinned photo diode to the FDs. The signal charges Q_3 and Q_4 stored in FD3 and FD4 are expressed as

$$Q_3 = Q_4 = I_{BL} R_D T_C \tag{6}$$

The background light cancelling is done by the subtraction of back-ground-only signals from the signals with received signal lights. In this case, Q_1 and Q_2 are TOF-dependent signals and Q_3 and Q_4 are background-only signals. The equation for estimating the range in each pixel is given by

$$L = \frac{1}{2} c T_d = \frac{1}{2} c T_0 \cdot \frac{Q_2 - Q_4}{Q_1 + Q_2 - 2Q_4} \tag{7}$$

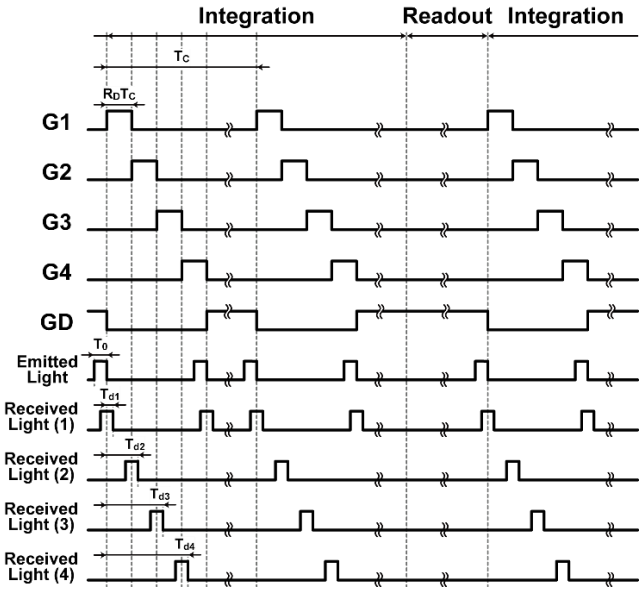

Fig 1: Timing diagram for the lock-in pixel operation using double pulses

$0 < TOF < R_D T_C$	$TOF = T_0 \frac{Q_1 - Q_3}{Q_1 + Q_4 - 2Q_3}$
$R_D T_C < TOF < 2R_D T_C$	$TOF = R_D T_C + T_0 \frac{Q_2 - Q_4}{Q_2 + Q_1 - 2Q_4}$
$2R_D T_C < TOF < 3R_D T_C$	$TOF = 2R_D T_C + T_0 \frac{Q_3 - Q_1}{Q_3 + Q_2 - 2Q_1}$
$3R_D T_C < TOF < 4R_D T_C$	$TOF = 3R_D T_C + T_0 \frac{Q_4 - Q_2}{Q_4 + Q_3 - 2Q_2}$

Fig 2: Range shift operation for extending the measurement range using shifted short double light pulses

Range Measurement with Range Switching by Thresholding

The timing diagram for the advanced range-shift operation is shown in Fig. 3. To produce range image, it is divided into 3 measurable ranges which are R1, R2 and R3. The proposed method calculates the difference of the 2 outputs in the 4-tap pixel outputs as given by equation (8) and (9). The two differential signals S_{13} and S_{24} changes like triangular wave to the TOF. By using this two signals, it is possible to measure the distance with the simple equations while automatically detecting the range zone. Also, equation (10) is the total of the absolute value of equation (8) and equation (9). S_A is the constant value proportional to the signal light intensity at the effective range zones. At the all zones, it will be calculated the range images by using the relative value of S_{13} , S_{24} for S_A. Also, setting the boundary of the range zone to a linearly changing point makes it possible to prevent an error in the distance even if an error occurs in the zone detection. Therefore, it will be expected high range linearity at wide range.

$$S_{13} = S_1 - S_3 \quad (8)$$

$$S_{24} = S_2 - S_4 \quad (9)$$

$$S_A = |S_{13}| + |S_{24}| \quad (10)$$

By calculating the difference value, the background light components can be removed and effective signal components can be left. While the conventional method needs three signals to remove background light components, the advanced method uses two signals for it. So, the time of calculating ADC and the area of analog circuit will be reduced.

Also, the equation for estimating the range is given by

$$D = D_{max0}\{D_1 Z_1 + D_2 Z_2 + D_3 Z_3\}E \quad (11)$$

where D_{max0} is the maximum range at one time-window, D_1 and D_2 and D_3 are each range equation, Z_1 and Z_2 and Z_3 and E are the digital value to determine correct regions. The timing diagram in the advanced range shift method is shown in Fig.3. And, the equations and values of determining the regions automatically is shown in Fig.4. The ingenuity is required to distinguish between the vicinity of the distance of zero and the vicinity of the maximum distance when distance is calculated using S_{13} and S_{24} by the range shift method. Then, we have setting threshold voltage to vanish the ambiguity. Therefore, effective measurement range will be reduced by using threshold voltage. But, it is very important to vanish the ambiguous regions. So, we need to set threshold voltage T to be sufficiently small value. While the conventional method is divided into 4 regions and there are no methods to determine correct regions automatically, the advanced method is reduced to 3 regions and is able to determine correct regions automatically.

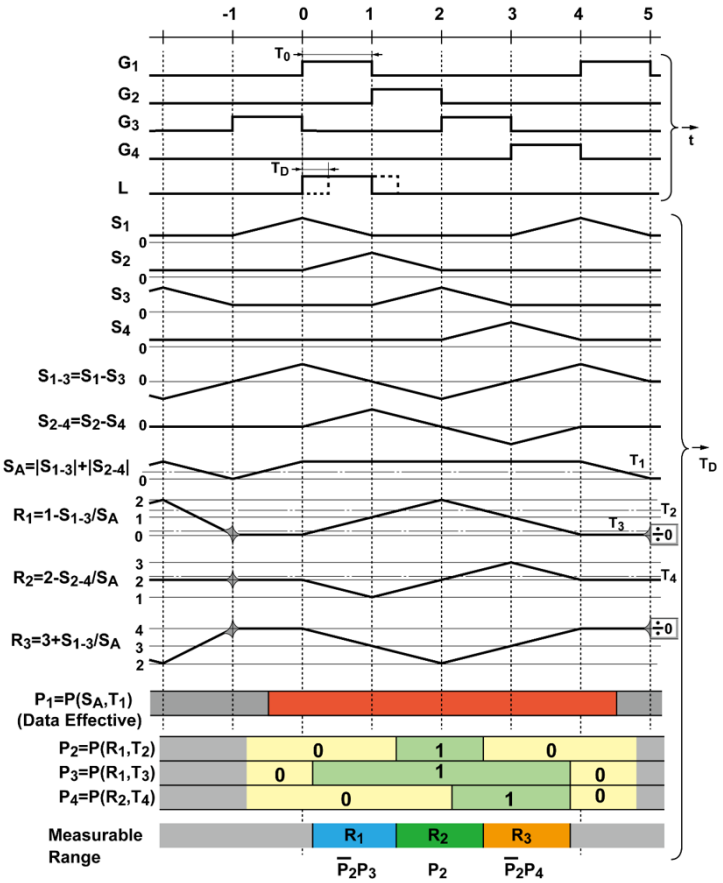

Fig3:Timing diagram for the lock-in pixel operation using advanced range shif t method

$D_1 = 1 - \frac{S_{13}}{S_A}$	$D_2 = 2 - \frac{S_{24}}{S_A}$	$D_3 = 3 + \frac{S_{13}}{S_A}$
$Z_1 = \overline{P_2}P_3$	$Z_2 = P_2$	$Z_3 = \overline{P_2}P_4$
$P_2 = \begin{cases} 1 (\text{if } R_1 \geq T_2) \\ 0 (\text{if } R_1 < T_2) \end{cases}$	$P_3 = \begin{cases} 1 (\text{if } R_1 \geq T_3) \\ 0 (\text{if } R_1 < T_3) \end{cases}$	$P_3 = \begin{cases} 1 (\text{if } R_1 \geq T_3) \\ 0 (\text{if } R_1 < T_3) \end{cases}$
$E = \begin{cases} 1 (\text{if } S_A \leq T_2) \\ 0 (\text{if } S_A > T_2) \end{cases}$		

Fig4:The equations of selecting the measurement range regions using advanced range shift method

Implemented TOF sensor

The block diagram of the TOF range imager is shown in Fig. 5. The TOF range imager consists of a 160×240 pixel array, vertical and horizontal shift register, ADC, and LEF charge modulator driver. Each pixel has four SF outputs which are shared by twelve charge modulators. Each of the four outputs from each pixel are connected each of the column ADC and are converted to digital codes in parallel using high-resolution folding integration/cyclic ADCs [11].

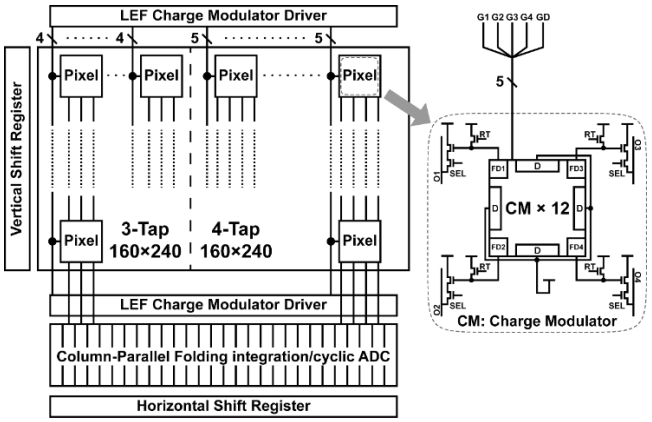

Fig5:Sensor architecture

Measurement Results

The signal light source is composed of 96 near-infrared LEDs with the 870nm wavelength, and the signal light pulse width T_0 is set to 15ns. An average power of the light source is 250mW. The cycle time of exposure T_C and the duty ratio R_D are 1.0μs and 0.015, respectively. The gate pulse width $R_D T_C$ for G1, G2, G3 and G4 is 15ns. In this measurement, T_0 of 15ns for the purpose of demonstration of high range resolution due to high-speed response of the pixel. The frame rate is 15.7fps. A lens with a focal length of 12.5mm and a F-number of 2.0 are mounted on the sensor. An infrared bandpass filter is placed in front of the lens. The High level for gate voltage of G1, G2, G3 and G4 is set to 2.5V, and the Low level is set to -1.0V. The High level for gate voltage of GD is set to 3.6V, and the Low level is set to -1.0V. The measured results are obtained by the average of 30 frames of raw data in 10×10 pixels in the center of the pixel array. We have used a white flat panel as an object.

Fig.6 shows a measured distance linearity and nonlinearity error. A white flat panel is located between 0.8m and 8.6m with the step of 0.2m. The results are compensated for the slop and offset. The slop is calibrated by the demodulation contrast, the offset is calibrated by the time offset. As the result, it confirms high range linearity even at the boundary of each zone. And, the nonlinearity error which is the difference of the measured range from real range is less than 2.2% of the full scale between 0.8m and 8.6m.

Fig.7 shows the measured range resolution by using advanced range shift method and conventional method without range shift. In the conventional method, both the gate pulse width and the light pulse width set up 60ns and the results are measured at the only one zone of Gate1 and Gate2. In the advanced method, both the gate pulse width and the light pulse width set up 15ns and the results are measured at the 3zone of Gate1, Gate2, Gate3 and Gate4. The range resolution is the standard derivation of the temporal deviation of measured range. The high range resolution of 95.9mm is achieved at 8.6m by using advanced range shift method. And, the range resolution of the advanced method is 3 times lower than that of the conventional method without range shift.

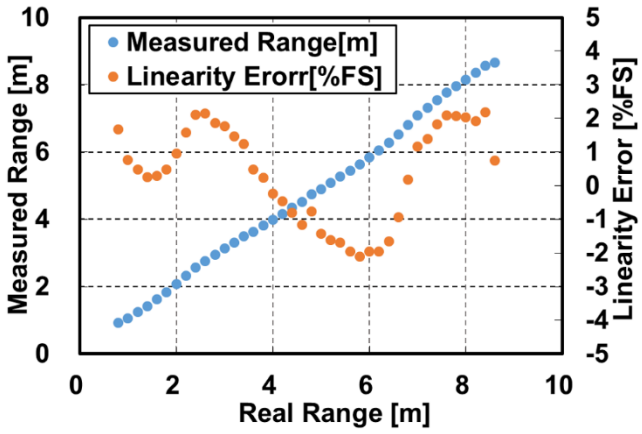

Fig6:Measured linearity and nonlinearity

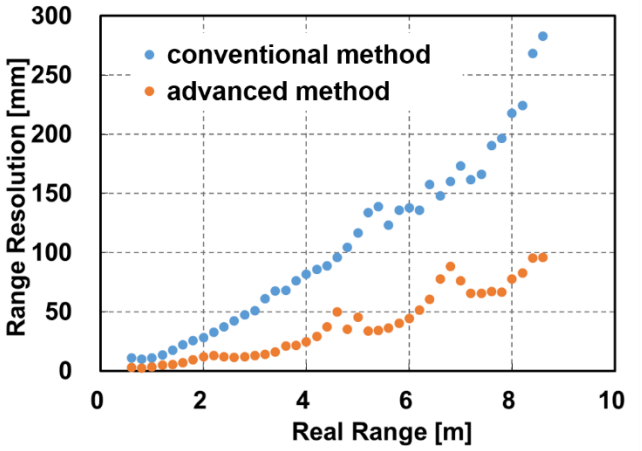

Fig7:Measured range resolution

Conclusion

This paper presented the advanced distance measurement method with range switching by thresholding. The proposed method uses the difference value of two pixel outputs and makes it possible to detect range zone by using the threshold voltage

automatically. Therefore, the background light components can be removed and effective signal components can be left before measuring distance. Also, it has succeeded high range linearity at the wide range. The nonlinearity error which is the difference of the measured range from real range is less than 2.2% of the full scale between 0.8m and 8.6m. The high range resolution of 95.9mm is achieved at 8.6m by using advanced range shift method. Compared with the conventional method without range shift, the range resolution of the advanced method is 3 times better than that of the conventional method. Table 1 summarizes the specification and characteristics of this work.

Acknowledgements

This study was partly supported by A JSPS KAKENHI Grant Number JP25220905, 25109003 and the Center of Innovation Program and Regional Innovation Ecosystem Program. The chip design was also supported by VLSI Design and Education Center (VDEC), the University of Tokyo in collaboration with Mentor Graphics, Inc. The authors appreciate Dongbu HiTek for CIS fabrication.

Table 1: Sensor specification

Process	0.11 μm 1P4M CIS
Total area	9.0 mm (H) x 9.3 mm (V)
Power supplies	1.5 V (Digital), 3.3 V (Analog, Digital)
Emitter	96 LED array with 870 nm wavelength
Lens	F# 2.0 / focal length of 12.5mm
Number of pixels	160 (H) x 240 (V) (4-Tap pixels)
Pixel size	22.4 μm (H) x 16.8 μm (V)
Conversion Gain	1.1 μV/e^-
Fill factor	41 % (with micro lens)
Frame rate	15.7 fps (exposure time of 50ms)
Modulation speed	15 ns (Light width) 15 ns (Gate width)
Demodulation Contrast	68.7% @15ns (Gate width)
Measured range	0.8 ~ 8.6 m
Non linearity	2.2 %FS
Range resolution	95.9mm @ 8.6m

References

[1] R. Lange, P. Seitz, A. Biber and S. Lauxtermann, "Demodulation Pixels in CCD and CMOS technologies for Time-of-Flight Ranging," Proc. SPIE, vol.3965, pp. 177-188, 2000.

[2] S. Kawahito, I. A. Halin, T. Ushinaga, T. Sawada, M. Homma, and Y. Maeda, "A CMOS time-of-flight range image sensor with gates-on-field-oxide structure," IEEE Sensors J., vol. 7, no.12, pp. 1578-1586, Dec. 2007.

[3] D. Stoppa, N. Massari, L. Pancheri, M. Malfatti, M. Perenzoni, and L. Gonzo, "A Range Image Sensor Based on 10um Lock-In Pixels in 0.18um CMOS Imaging Technology," IEEE J. Solid-State Circuits, vol. 46, no.1, pp. 248-258, Jan. 2011.

[4] S. J. Kim, B. Kang, K. D. K. Kim, K. Lee, C. Y. Kim, and K. Kim, "A 1920x1080 3.65μm-pixel 2D/3D image sensor with split and binning pixel structure in 0.11 μm standard CMOS," ISSCC Dig. Tech. Papers, pp. 396-397, Feb. 2012.

[5] O. Shcherbakova, L. Pancheri, G.-F. Dalla Betta, N. Massari, and D. Stoppa, "3D camera based on linear-mode gain-modulated avalanche photodiodes," ISSCC Dig. Tech. Papers, pp. 490- 491, Feb. 2013.

[6] A. Payne, A. Daniel, A. Mehta, B. Thompson, C. S. Bamji, D. Snow, H. Oshima, L. Prather, M. Fenton, L. Kordus, P. O'Connor, R. McCauley, S. Nayak, S. Acharya, S. Mehta, T. Elkhatib, T. Meyer, T. O'Dwyer, T. Perry, V.-H. Chan, V. Wong, V. Mogallapu, W. Qian, and Z. Xu, "A 512×424 CMOS 3D Time-of-Flight image sensor with multi-frequency photo-demodulation up to 130MHz and 2GS/s ADC," ISSCC Dig. Tech. Papers, pp. 134-135, Feb. 2014.

[7] Dal Mutto, C.; Zanuttigh, P.; Cortelazzo, G.M. "Time-of-Flight Cameras and Microsoft Kinect™," Springer Science & Business Media: New York, NY, USA, Jan. 2013.

[8] Y.Kato, T.Sano, Y.Moriyama, S.Maeda, T.Yamazaki, A.Nose, K.Shina, Y,Yasu, W.Tempel, and A.Ercan, "320x240 Back-Illuminated 10μm CAPD Pixels for High Speed Modulation Time-of-Flight CMOS Image Sensor," VLSI Circuits, 2017 Symposium on, Jon. 2017.

[9] S. Kawahito, G. Beak, Z. Li, S.-M. Han, M.-W. Seo, K. Yasutomi, and K. Kagawa, "CMOS Lock-in Pixel Image Sensors with Lateral Eelectric Field Cotrol for Time-Resolved Imaging," Proc. 2013 Int. Image Sensor Workshop (IISW), pp. 361-364, Jun. 2013.

[10] S.-M. Han, T. Takasawa, T. Akahori, K. Yasutomi, K. Kagawa, and S. Kawahito, "A 413×240-pixel sub-centimeter resolution Time-of-Flight CMOS image sensor with in-pixel background canceling using lateral-electric-field charge modulators," ISSCC Dig. Tech. Papers, pp. 130-131, Feb. 2014.

[11] M.-W. Seo, S.-H. Suh, T. Iida, T. Takasawa, K. Isobe, T. Watanabe, S. Itoh, K. Yasutomi, and S. Kawahito, "A Low-Noise High Intrascene Dynamic Range CMOS Image Sensor With a 13 to 19b Variable-Resolution Column-Parallel Folding-Integration/Cyclic ADC," IEEE J. Solid-State Circuits, vol.47, no.1, pp. 272-283, Jan. 2012.

[12] T.Kasugai,et al., "A time-of-flight CMOS range image sensor using 4-tap output pixels with lateral-electric-field control," Electronic Imaging 2016, Feb. 2016

Author Biography

Mr.Kohei Yamada was received the B.E. degrees in from Shizuoka University, Hamamatsu Japan, in 2017. He is now a master course student of Shizuoka University.